Front. Biol. 2015, 10(3): 279–286
DOI 10.1007/s11515-015-1344-4

RESEARCH ARTICLE

Comparative study of oxidative stress induced by sand flower and schistose nanosized layered double hydroxides in N2a cells

Yu Lu[1,*], Biao Yan[1,*], Xudong Liu[1], Yuchao Zhang[1], Shibi Zeng[2], Hao Hu[2], Rong Xiang[3], Yu Xu[3], Ying Yu[2], Xu Yang (✉)[1]

[1] *Hubei Key Laboratory of Genetic Regulation and Integrative Biology College of Life Science, Central China Normal University, Wuhan 430079, China*
[2] *Institute of Nanoscience and Nanotechnology, Central China Normal University, Wuhan 430079, China*
[3] *Department of Otolaryngology, Head & Neck Surgery, Renmin Hospital of Wuhan University, Wuhan 430060, China*

Abstract **Magnesium–aluminum layered double hydroxide (Mg/Al–LDH) nanoparticles have strong potential application as drug delivery systems because of their low toxicity and suitable biocompatibility. However, few studies have described the morphological effects of these hydroxides on nerve cells. The present study compares the oxidative stress induced by different concentrations (i.e., 0, 50, 100, 200, 400, and 800 μg/mL) of sand flower and flake nano-Mg/Al–LDHs in mouse neuroblastoma cells (N2a) when these cells were exposed for 24 and 48 h. Cell viability was detected by MTT assay, and production of reactive oxygen species (ROS), glutathione (GSH), and malondialdehyde (MDA) were monitored to evaluate oxidative damage. Results suggested that sand flower nano-LDHs, at the appropriate concentrations (less than 200 μg/mL), especially those of about 100–200 nm in size, induce no harmful effects on N2a cells.**

Keywords magnesium–aluminum layered double hydroxide, mouse neuroblastoma cell, oxidative stress, reactive oxygen species

Introduction

Rapid developments in nanomedicine, which refers to the application of nanotechnology to medicine, has promoted the use of nanoparticle-scale therapeutic carriers (Wang et al., 2012). Drug delivery using nanoparticles, which present several advantages, including small size, surface targeting, easy uptake by cells through the tissue matrix, and potential to cross the blood-brain barrier (BBB), is a popular research field (De Jong and Borm, 2008). Layered double hydroxides (LDHs) for cellular delivery of anionic drugs and other biofunctional molecules have recently attracted increased interest from the scientific community because of their low toxicity, suitable biocompatibility, high stability, pH-dependent solubility, and enhanced cellular uptake behavior (Chakraborty et al., 2013). LDH-mediated drug delivery can also help overcome drug resistance (Hesse et al., 2013). Besides reducing multi-drug resistance and overcoming the BBB, drug release by LDHs can be controlled so that the drug is delivered within a predetermined time from the nanoparticles to a target organ at the effective concentration. Nanoparticles thus have broad application prospects as a new medically controllable release system (Akhter et al., 2013).

Tailor-made nanomaterials have the potential to cross the BBB and may present new routes for drug delivery into the brain (De Jong and Borm, 2008). Some studies have shown that nano-LDHs can be effectively used as a drug carrier because they increase the water solubility of the drug, effectively control drug release, and improve drug efficiency (Li et al., 2004; Tyner et al., 2004). Thus, LDHs can function as a biocompatible delivery matrix for various drugs and facilitate a significant increase in drug delivery efficiency (Li et al., 2010).

LDHs are considered new generation materials that comprise a two-dimensional layered structure similar to that

Received September 2, 2014; accepted January 5, 2015
Correspondence: Xu Yang
E-mail: yangxu@mail.ccnu.edu.cn

*These authors contributed equally to this work.

of the mineral brucite, $Mg(OH)_2$ (Rives, 2002). The chemical composition of LDH can be represented by the general formula $[M^{2+}_{1-x}M^{3+}_{x}(OH)_2]^{x+}[A^{n-}]_{x/n}\cdot mH_2O$, where M represents a metal cation and A^{n-} is an exchangeable anion in the interlayer space; here, x is the resultant charge imbalance in the structure and m is the number of structural water molecules in the LDH interlayer (Chakraborty et al., 2013). Magnesium–aluminum LDHs (Mg/Al–LDH) derived from LDH calcination are a good reservoir for different types of drugs in their anionic form and particular interesting materials in the field of cellular delivery of drugs and biomolecules (Chakraborty et al., 2012).

Although the shape or morphology of a nanocarrier performs important functions in drug transport to specific cells or tissues and subsequent endocytosis within cellular compartments (Chakraborty et al., 2012), the effects of shape on nerve cells have not been evaluated to reveal the mechanism of morphology evolution during targeting of specific cells or tissues. While a few reports focusing on morphological effects (Zeng et al., 2013) have been published, no resulting damage has yet been shown. Besides several other environmental or genetic factors, oxidative stress (OS) leading to free radical attack of neural cells contributes to neuro-degeneration (Del Hoyo, 2007). Thus, OS is regarded as a key upstream event observed after nerve cell exposure to nanoparticles.

In the present study, two shapes of tailor-made nano-Mg/Al–LDHs (i.e., sand flower and schistose nano-LDHs) were evaluated in terms of OS induced in mouse neuroblastoma cells (N2a cells). N2a cells were selected as the model for this *in vitro* experiment because these cells are frequently used in biological research. The cells can help determine whether sand flower or schistose nano-LDHs are more suitable as drug carriers for human nerve cells. Evaluations were achieved by recording cell morphologies and measuring changes in reactive oxygen species (ROS), glutathione (GSH), and malondialdehyde (MDA) levels in N2a cells. Such changes may present significant implications for the targeted treatment of brain cells when nano-LDHs are prompted to cross various biological barriers within the body for drug delivery.

Materials and methods

Reagents and apparatus

The LDH nanocomposites used in this study were provided by the Institute of Nanoscience and Nanotechnology, Central China Normal University. RPMI 1640 medium (Gibco, Life Technologies, Grand Island, NY, USA), fetal calf serum (Gibco), 3-(4,5-dimethylthiazol-2-yl)-2,5-diphenyltetrazolium bromide (MTT), Hoechst 33258, 2,7-dichlorodihydrofluorescein diacetate (DCFH-DA), 2-thiobarbituric acid (TBA), and 3-carboxy-4-nitrophenyl disulfide (DTNB) were purchased from Sigma-Aldrich (St. Louis, MO, USA). All other chemicals used were of the highest grade available commercially.

A CO_2 incubator (Thermo Fisher Scientific, Waltham, MA, USA), superclean bench (Suzhou, China), low-temperature refrigerated centrifuge (Eppendorf-5417R), Nikon Eclipse TE2000-S microscope, continuous-wave and fluorescent microplate spectrophotometer (Bio-teck FLX800, USA), fluorescence spectrophotometer (Hitachi F-4500, Japan), and scanning electron microscope (SEM, JSM-6700F, Japan) were used in this study.

Preparation of Mg/Al–LDHs and characterization

Based on a study conducted by Zeng et al. (2013), LDH nanocomposites with sand flower and dense layered morphologies were prepared by the co-precipitation method at pH = 10 under different conditions with stirring. The SEM images of the sand flower and schistose LDH nanocomposites were observed using a JSM-6700F microscope (Japan).

Cell culture and exposure to Mg/Al–LDHs

Nano-Mg/Al–LDHs were dispersed in complete culture medium. Based on previous repeated studies in our laboratory, Mg/Al–LDH concentrations of 50, 100, 200, 400, and 800 μg/mL were chosen. These concentrations are also in accordance with the work of Li et al. (2010). Considering the dispersibility of LDHs in medium, all suspensions were sonicated for 20 min at a frequency of 40 kHz at 20 °C before inoculation into cells (Wen et al., 2013).

N2a cells were cultured in RPMI 1640 medium supplemented with 10% fetal calf serum and then incubated in medium containing different concentrations of the nanocomposites at 37 °C in a humidified atmosphere with 5% CO_2 for 24 and 48 h. For the intracellular ROS generation, GSH depletion, and MTT assays, cells were seeded into 96-well plates at a density of 1×10^4 cells/well. MDA assay was performed with a cell density of 1×10^5 cells/well in 24-well plates.

Cell morphology examinations

N2a cells were cultured in various concentrations of Mg/Al–LDHs, as previously described. After 24 h of exposure, cells were quickly washed twice with PBS to remove particles and then fixed with 4% paraformaldehyde in PBS for 1 h at room temperature. This procedure was adopted from Roualdes et al. (2010). Cells were observed using a microscope.

MTT assay

MTT assay was used to reveal the cell viability induced by different concentrations of Mg/Al–LDH nanocomposites at exposure times of 24 and 48 h. In this assay, the method of Li et al. (2010) was followed.

Intracellular ROS generation assay

The OS process is capable of generating ROS. ROS levels were measured by monitoring increases in the fluorescence intensity of DCF using a previously described procedure with minor modifications according to the method of Ma et al. (2014).

GSH depletion assay

GSH, a thiol, is the major scavenger of intracellular ROS. GSH contains sulfhydryl, which can react with DTNB to produce yellow compounds in the dark (Anderson, 1985). GSH content was examined by determining DTNB fluorescence in each well of the culture plates following the method of Wen et al. (2013).

MDA determination assay

MDA is produced by lipid peroxidation. MDA can react with TBA, thereby resulting in a stable chromophoric product at high temperatures (90–100 °C). The concentration of MDA can be measured colorimetrically at 530–540 nm under acidic conditions. In this procedure, the method of Ma et al. (2012) was strictly followed.

Statistical analyses

Data are presented as mean ± standard error and analyzed and plotted using Origin 6.1 software (OriginLab, Berkeley, CA, USA). One-way ANOVA combined with Tukey's test was used to determine the significance of differences between groups. p values less than 0.05 and 0.01 were used to evaluate statistical significance.

Results

Characterization of nanosized-Mg/Al–LDHs (Mg/Al = 3:1)

The effectiveness of nano-LDHs for drug delivery is highly related to their size and structure; thus, these parameters were examined by SEM in this work. Based on a study conducted by Zeng et al. (2013), LDHs with sand flower and dense layered morphologies may be prepared by the co-precipitation method at pH = 10 under different conditions with and without stirring. Without stirring, the nanoflakes were more likely to be deposited randomly. When the stirring power was suitable, the nature of the flakes to form a sand flower morphology could be resisted. Sand flower clusters with diameters of approximately 0.5 μm consisted of nanoflakes interwoven with each other to form a porous network (Fig. 1A). The slightly curved nanoflakes were approximately 200–400 nm wide and 10 nm thick (Fig. 1B). Figure 1B shows that the nanoflakes are randomly deposited without stirring and that the composite structure is more compact than the sand flower nano-LDHs.

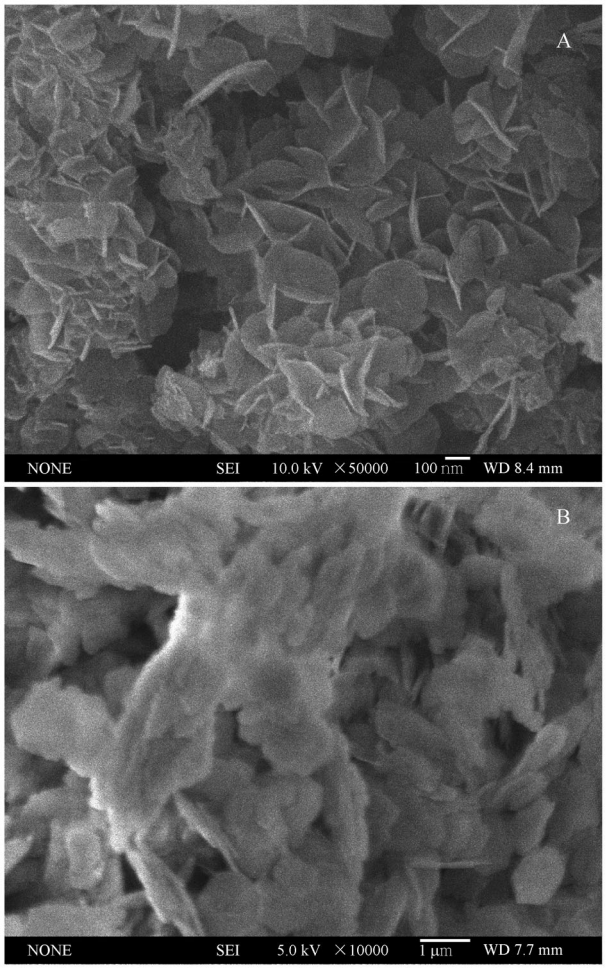

Figure 1 Scanning electron microscopic images of synthesized nano-LDHs. (A) Sand flower nano-LDHs and (B) schistose nano-LDHs.

Cell morphology in the presence of nano-LDHs

Visualization was employed to determine the influence of nano-LDHs on N2a cells (Fig. 2). LDH nanoparticles could be seen within and around the cells because these particles are easily endocytosed within the cellular compartments based on their size and morphology (Chakraborty et al., 2011). As the concentration of nano-LDHs increased, cell adhesion obviously increased. The dispersion of schistose nano-LDHs was much poorer than that of sand flower nano-LDHs.

MTT assay

MTT assay indicates the cell viability induced by different concentrations of nano-sized LDHs. As the concentration of flake nano-LDHs increased, cell viability significantly

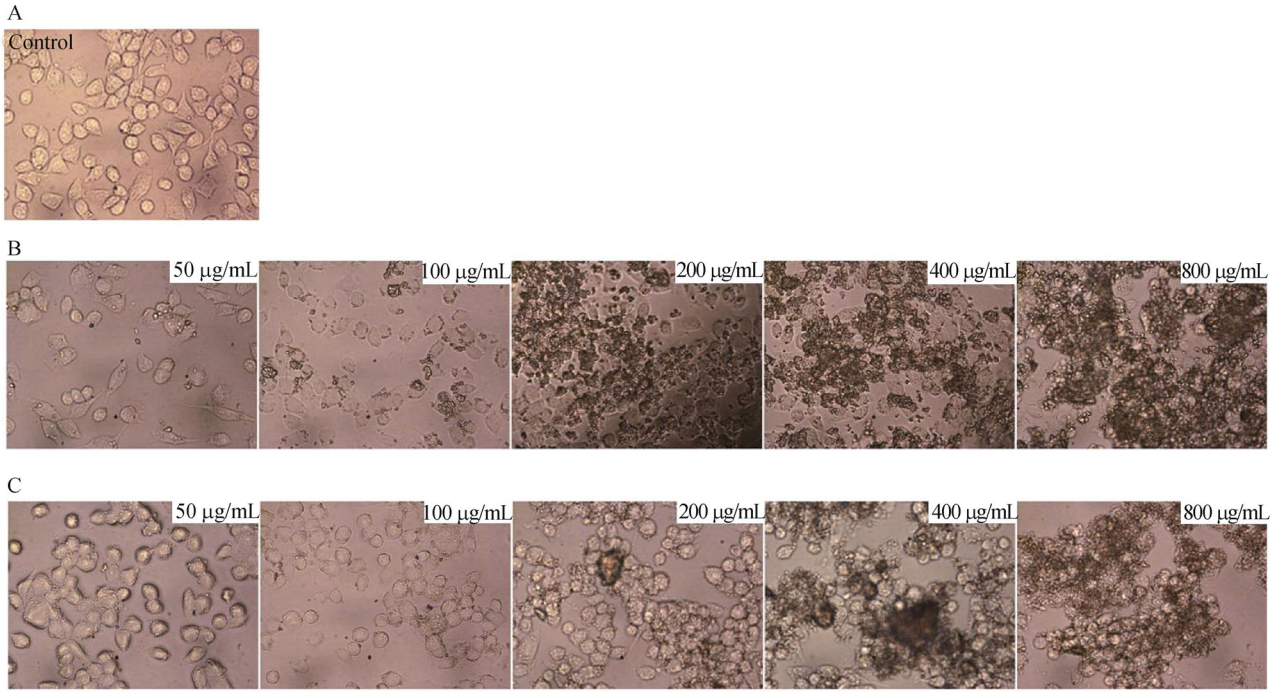

Figure 2 Morphological images of N2a cells exposed to nano-LDHs (stained with Hoechst 33258). The images are shown at 40× magnification. Row (A) shows N2a cells of the blank group. Row (B) shows images of N2a cells exposed to sand flower nano-LDHs at different concentrations (50, 100, 200, 400, and 800 μg/mL). Row (C) shows images of N2a cells exposed to schistose nano-LDHs at different concentrations (50, 100, 200, 400, and 800 μg/mL).

decreased. Significant differences in cell viability induced by the sand flower and flake nano-LDH groups were observed at concentrations greater than 50 μg/mL ($p < 0.01$; Fig. 3).

Intracellular ROS generation and GSH depletion

ROS are the most important biomarkers of OS, and GSH is a scavenging agent that can scavenge ROS molecules to prevent oxidation. The results of intracellular ROS generation among the groups are shown in Fig. 4. ROS levels at 24 h increased in sand flower nano-LDH groups as the nanoparticle exposure dose increased, although statistical significance compared with the control group was achieved only at 400 μg/mL ($p < 0.05$). By contrast, a significant increase in ROS was observed in the flake nano-LDH groups at 200 μg/mL ($p < 0.01$). Compared with the sand flower nano-LDH group at 800 μg/mL, the ROS levels of the flake group were significantly increased ($p < 0.05$) (Fig. 4A). As exposure time increased to 48 h, ROS contents decreased even if the rate at which ROS content increased remained unchanged (Fig. 4B). Nano-LDHs are thus considered to possess good biocompatibility. Production of excess ROS was not induced in the experimental groups compared with that in the control until LHD concentrations exceeded 200 μg/mL ($p < 0.05$).

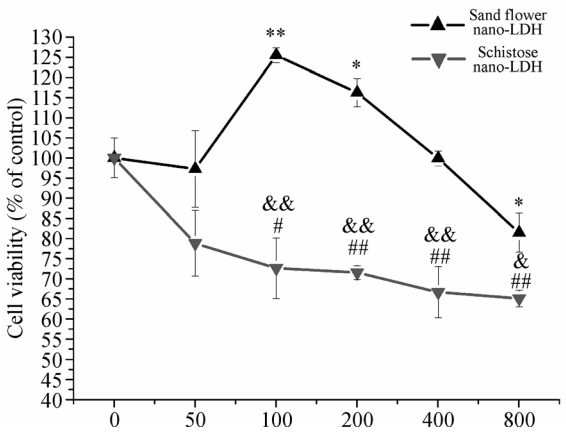

Figure 3 Effects of nano-LDHs on the viability of N2a cells ($n = 5$). * or #, $p < 0.05$. ** or ##, $p < 0.01$, compared with the control. &, $p < 0.05$; &&, $p < 0.01$, each sand flower nano-LDH group compared with the corresponding schistose nano-LDH group.

Figure 5 shows the relationship between GSH content and different concentrations of nano-LDHs. While high-dose (200 μg/mL) sand flower nano-LDHs led to a significant decrease in GSH levels after exposure for 24 h ($p < 0.05$) (Fig. 5A), no significant effects were observed at 48 h (Fig. 5B). Upon exposure to schistose nano-LDHs, however, significant changes in GSH content were observed ($p < 0.05$, $p < 0.01$) compared with the control group at both 24 and 48 h. GSH in N2a cells thus seem to be more vulnerable to schistose nano-LDHs than to sand slower nano-LDHs.

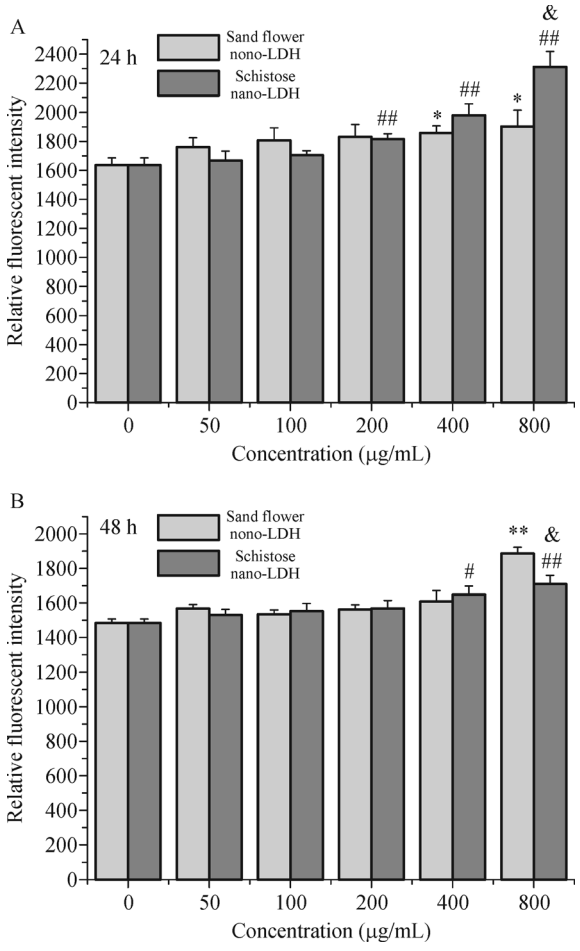

Figure 4 ROS levels in N2a cells ($n = 5$). (A) DCF fluorescence intensities induced by different concentrations of nano-LDH at 24 h. (B) DCF fluorescence intensities induced by different concentrations of nano-LDH at 48 h. * or #, $p < 0.05$; ** or ##, $p < 0.01$, compared with the control; &, $p < 0.05$, each sand flower nano-LDH group compared with the corresponding schistose nano-LDH group.

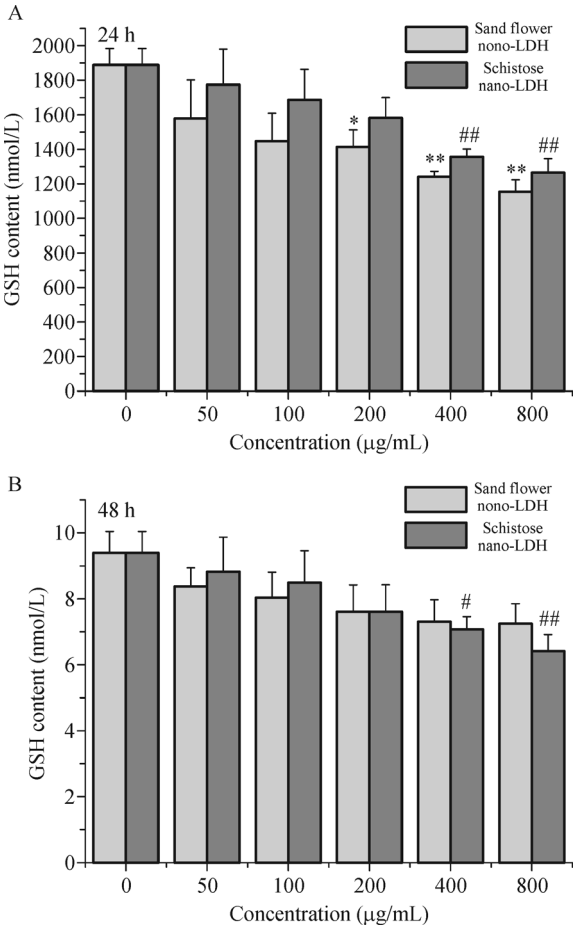

Figure 5 GSH levels in N2a cells ($n = 5$). (A) GSH contents induced by different concentrations of nano-LDHs at 24 h. (B) GSH contents induced by different concentrations of nano-LDHs at 48 h. * or #, $p < 0.05$; ** or ##, $p < 0.01$, compared with the control.

Intracellular lipid peroxidation

MDA is an end-product of peroxidation. Thus, changes in MDA concentration can indicate lipid peroxidation, which damages cell integrity. Lipid peroxidation occurred in the sand flower nano-LDH groups, particularly after exposure to the highest dosage (800 μg/mL) ($p < 0.05$) (Fig. 6A). Increases in schistose nano-LDH exposure dosage were associated with increases in MDA levels in N2a cells, as observed in the 400 and 800 μg/mL groups ($p < 0.05$) (Fig. 6A). Figure 6B shows that MDA content presents a significant relationship with the concentration and exposure time of nano-LDHs. Indeed, these results exhibit a certain dose-dependent relationship, which suggests the possibility that lipid peroxidation injury is induced by schistose nano-LDH, especially at doses of 400 and 800 μg/mL.

Discussion

Although a considerable amount of data on the toxicity of nano-LDHs are available (Ladewig et al., 2009), recent efforts have focused on the promising potential of drug delivery systems, and attempts to change their size and morphology have been made to improve their suitability as inorganic drug or gene delivery carriers. Depending on the requirements, the shape and size of nanocarriers can be tailored and the speed of delivery to specific targets can be adjusted (Chakraborty et al., 2011). The size and shape of nano-LDHs must be controlled to reduce multi-drug resistance development and avoid the BBB. Kwak et al. (2002) pointed out that nano-LDHs of 100–200 nm are appropriate for use as gene or drug delivery carriers. The nano-LDHs used in this study are approximately 100–400 nm long and 10–40 nm thick; such dimensions support their applicability in the field of biomedicine.

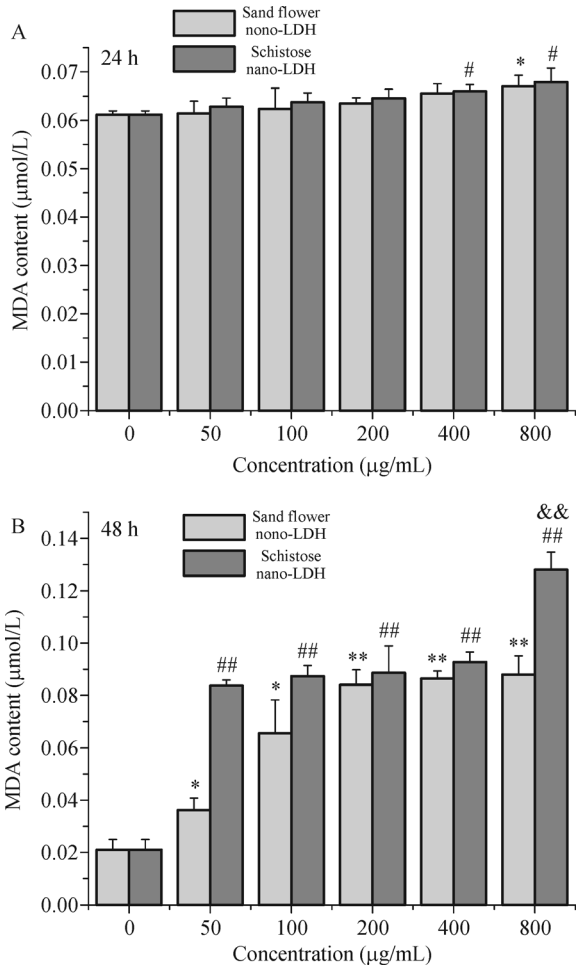

Figure 6 MDA levels in N2a cells ($n = 5$). (A) MDA contents induced by different concentrations of nano-LDHs at 24 h. * or #, $p < 0.05$, compared with the control. (B) MDA contents induced by different concentrations of nano-LDHs at 48 h. * or #, $p < 0.05$; ** or ##, $p < 0.01$, compared with the control. &&, $p < 0.01$, each sand flower nano-LDH group compared with the corresponding schistose nano-LDH group.

When N2a cells were cultured with nano-LDHs, cell morphology images showed an increase in cell adhesion. While the top panels (low-concentration exposure groups) appeared to show considerably fewer cells, this phenomenon is in fact related to the dispersion of the cells. Considering the whole area of the cultured cell, the number of cells in low-concentration groups was far greater than that in high-concentration groups, and increasing exposure concentration consistently decreased the number of bound cells. This seemingly contradictory phenomenon in the pictures may be explained by the fact that some nano-LDHs have higher adsorption capacity than others, thereby causing cells to accumulate in the surrounding area. By contrast, cells in low-concentration groups are uniformly dispersed because they are less affected by nano-LDHs. In other words, most cells in high-concentration groups accumulated around the NPs (nano-LDHs), while the others were prone to cell death. This result is consistent with the results of MTT assay. MTT detection assay was used to explore and compare the viability of N2a cells in different concentrations of nano-LDHs. The viability of cells upon exposure to nano-LDHs could be a good indication of their compatibility. Even at the maximum concentration (800 μg/mL), the viability of cells in the flake nano-LDH groups was close to 70% of the viability in the blank group. MTT assay indicated that cell viability is associated with succinate dehydrogenase in cellular mitochondria. Results showed that increases in cell viability in sand flower nano-LDH exposure groups (100 and 200 μg/mL) compared with those in the control group were statistically significant ($p < 0.01$, $p < 0.05$). Increases in absorbance (MTT assay) observed in sand flower nano-LDH groups were not caused by the increased proliferation of cells. Zhang et al. (2011) reported that this phenomenon can explain the increase in absorbance observed in NPs (nano-LDHs) because MTT salt is mainly reduced by dehydrogenases in mitochondria. The respiratory chain of mitochondria affected by NPs could also increase reduction of MTT salt. Such an event can explain the high cellular activity detected during the early stages of exposure that is not related to the increase in cell viability. In general, the viability of cells in the sand flower nano-LDH groups was significantly better than that of cells in the schistose groups under the same concentration. Numerous studies show that the viability of nano-LDHs is rarely involved in OS; in terms of detection of a series of biomarkers, including ROS, GSH, and MDA, however, cell viability may be related to the oxidative damage induced by nano-LDHs.

ROS levels observed after 24 h of treatment increased in a concentration-dependent manner (Fig. 4A). With increasing exposure concentration, high-dose nano-LDH groups (> 200 μg/mL) showed a significant increase in ROS levels and decreases in cell viability and GSH levels. As exposure time increased to 48 h, cell death inevitably occurred. As well, while the rate at which ROS content increased remained unchanged, ROS content decreased (Fig. 4B). Nano-LDHs are thus considered to possess good biocompatibility. Excess ROS was not induced among the experimental groups compared with the control group until the nano-LDH concentration was greater than 200 μg/mL ($p < 0.05$, $p < 0.01$). Decreased GSH levels were detected in accordance with the increase in ROS levels (Fig. 5). Besides a significant reduction in GSH levels in the 200 μg/mL group compared with that in the control group ($p < 0.05$) (Fig. 5A), a decrease in GSH was also observed after treatment for 48 h (Fig. 5B). Similarly, a decrease in GSH was observed with the simultaneous increase in ROS level. These phenomena may be explained by the fact that increased exposure times inevitably lead to cell death and that intracellular oxidative damage promotes an imbalance in ROS and GSH levels (Ma et al., 2014). Figure 6 shows that MDA levels are higher in cells treated for 48 h than in cells treated for only 24 h. This trend directly contrasts observed ROS and GSH levels, which

continued to increase with exposure time. Variations observed may be attributed to the fact that MDA assay was used to detect the extent of cell membrane damage. When the cell membrane adheres to the growing NPs, the MDA contents of the cells increase and cell damage occurs extensively.

OS is a well-defined paradigm that can explain toxic effects induced by nanomaterials (Li et al., 2010; Ma et al., 2012). The OS process produces ROS, which are well-known toxic agents at elevated levels. When produced in excess, ROS can cause tissue injury. Tissue injury itself can cause ROS generation (Ma et al., 2014). Research results show that ROS generation during the oxidation process is an important cause of biological toxicity of nanomaterials (Nel et al., 2006) and that nanoparticles can also generate ROS (Kim et al., 2010). The results described above show that the oxidative and reductive balance change only when the nano-LDH concentration is greater than 200 μg/mL. Cells in such conditions could potentially be susceptible to OS (Ma et al., 2012). An imbalance between ROS and GSH is particularly evident when excess ROS and reduced GSH levels, especially in the 800 μg/mL group, were combined. In this case, MDA is produced as a result of lipid peroxidation. The results of this study show that nano-LDHs induce increases in ROS and MDA levels and decreases in GSH levels as the nanoparticle dosage increases. OS leading to free radical attack on N2a cells contributing to cell injury likely causes these changes.

Despite the wide availability of studies on the controllable preparation of LDHs, few reports have focused on the morphological effects induced by these compounds (Zeng et al., 2013). The experimental data reveal that sand flower nano-LDH is superior to nano-schistose LDH as a relatively safe drug carrier with improved biocompatibility and low toxicity. Nonetheless, the effects of high dosages of these LDHs must be considered in practical application. Although drug delivery efficiency increased as the LDH content increased, safe application considerations must not be ignored when attempting to maximize therapeutic activity by increasing LDH content. The results described above demonstrate that nano-LDHs could induce lipid damage at concentrations higher than 200 μg/mL. Thus, an LDH concentration of less than 200 μg/mL appears to be an acceptable dosage for relatively safe application. As this study focused only on cellular experiments, further *in-vivo* studies with mice are necessary to confirm the drug delivery efficiency and biocompatibility observed in the LDHs. Our next study will focus on these topics.

Conclusion

ROS, GSH, MDA, and MTT assays were used to evaluate and compare the cytotoxicity induced by different concentrations of sand flower and schistose nano-LDHs in N2a cells. The results suggested that sand flower nano-LDHs are more suitable as drug delivery vehicles than schistose nano-LDH. At the appropriate concentration (less than 200 μg/mL), sand flower nano-LDHs present better biocompatibility and lower toxicity than schistose nano-LDHs.

Acknowledgements

This work was supported by the National Natural Science Foundation of China (Grant No. 51136002) and the 12th Five-Year Key Program for Science and Technology Development of China (No. 2012BAJ02B0301).

Compliance with ethics guidelines

Yu Lu, Biao Yan, Xudong Liu, Yuchao Zhang, Shibi Zeng, Hao Hu, Rong Xiang, Yu Xu, Ying Yu, and Xu Yang declare that they have no conflicts of interests. This article does not contain any studies related to human or animal subjects performed by any of the authors.

References

Akhter S, Ahmad I, Ahmad M Z, Ramazani F, Singh A, Rahman Z, Ahmad F J, Storm G, Kok R J (2013). Nanomedicines as cancer therapeutics: current status. Curr Cancer Drug Targets, 13(4): 362–378

Anderson M E (1985). Determination of glutathione and glutathione disulfide in biological samples. Methods Enzymol, 113: 548–555

Chakraborty J, Roychowdhury S, Sengupta S, Ghosh S (2013). Mg-Al layered double hydroxide-methotrexate nanohybrid drug delivery system: evaluation of efficacy. Mater Sci Eng C Mater Biol Appl, 33 (4): 2168–2174

Chakraborty M, Dasgupta S, Sengupta S, Chakraborty J, Ghosh S, Ghosh J, Mitra M K, Mishra A, Mandal T K, Basu D (2012). A facile synthetic strategy for Mg–Al layered double hydroxide material as nanocarrier for methotrexate. Ceram Int, 38(2): 941–949

De Jong W H, Borm P J (2008). Drug delivery and nanoparticles: applications and hazards. Int J Nanomedicine, 3(2): 133–149

Del Hoyo C (2007). Layered double hydroxides and human health: an overview. Appl Clay Sci, 36(1): 103–121

Hesse D, Badar M, Bleich A, Smoczek A, Glage S, Kieke M, Behrens P, Müller P P, Esser K H, Stieve M, Prenzler N K (2013). Layered double hydroxides as efficient drug delivery system of ciprofloxacin in the middle ear: an animal study in rabbits. J Mater Sci Mater Med, 24(1): 129–136

Kim I S, Baek M, Choi S J (2010). Comparative cytotoxicity of Al_2O_3, CeO_2, TiO_2 and ZnO nanoparticles to human lung cells. J Nanosci Nanotechnol, 10(5): 3453–3458

Kwak S Y, Jeong Y J, Park J S, Choy J H (2002). Bio-LDH nanohybrid for gene therapy. Solid State Ion, 151(1): 229–234

Ladewig K, Xu Z P, Lu G Q (2009). Layered double hydroxide nanoparticles in gene and drug delivery. Expert Opin Drug Deliv, 6 (9): 907–922

Li B, He J, Evans G (2004). Inorganic layered double hydroxides as a drug delivery system—intercalation and *in vitro* release of fenbufen. Appl Clay Sci, 27(3): 199–207

Li Y, Liu D, Ai H, Chang Q, Liu D, Xia Y, Liu S, Peng N, Xi Z, Yang X (2010). Biological evaluation of layered double hydroxides as efficient drug vehicles. Nanotechnology, 21(10): 105101

Ma P, Luo Q, Chen J, Gan Y, Du J, Ding S, Xi Z, Yang X (2012). Intraperitoneal injection of magnetic Fe_3O_4-nanoparticle induces hepatic and renal tissue injury via oxidative stress in mice. Int J Nanomedicine, 7: 4809–4818

Ma P, Yan B, Zeng Q, Liu X, Wu Y, Jiao M, Liu C, Wu J, Yang X (2014). Oral exposure of Kunming mice to diisononyl phthalate induces hepatic and renal tissue injury through the accumulation of ROS. Protective effect of melatonin. Food Chem Toxicol, 68: 247–256

Nel A, Xia T, Mädler L, Li N (2006). Toxic potential of materials at the nanolevel. Science, 311(5761): 622–627

Rives V (2002). Characterisation of layered double hydroxides and their decomposition products. Mater Chem Phys, 75(1-3): 19–25

Roualdes O, Duclos M E, Gutknecht D, Frappart L, Chevalier J, Hartmann D J (2010). *In vitro* and *in vivo* evaluation of an alumina-zirconia composite for arthroplasty applications. Biomaterials, 31(8): 2043–2054

Tyner K M, Schiffman S R, Giannelis E P (2004). Nanobiohybrids as delivery vehicles for camptothecin. J Control Release, 95(3): 501–514

Wang A Z, Langer R, Farokhzad O C (2012). Nanoparticle delivery of cancer drugs. Annu Rev Med, 63(1): 185–198

Wen H, Zhong J, Shen B, Gan T, Fu C, Zhu Z, Li R, Yang X (2013). Comparative study of the cytotoxicity of the nanosized and microsized tellurium powders on HeLa cells. Front Biol, 8(4): 444–450

Zeng S, Xu X, Wang S, Gong Q, Liu R, Yu Y (2013). Sand flower layered double hydroxides synthesized by co-precipitation for CO_2 capture: Morphology evolution mechanism, agitation effect and stability. Mater Chem Phys, 140(1): 159–167

Zhang Y F, Phila M, Zheng Y F, Qin L (2011). A comprehensive biological evaluation of ceramic nanoparticles as wear debris. Nanotechnology. Biol Med (Paris), 7(6): 975–982